ADVANCES IN ATMOSPHERIC SCIENCES, VOL. 32, MAY 2015, 601–612

Role of the Subtropical Westerly Jet Waveguide in a Southern China Heavy Rainstorm in December 2013

LI Chun[1,2] and SUN Jilin*[1]

[1]*Physical Oceanography Laboratory, Qingdao Collaborative Innovation Center of Marine Science and Technology, Key Laboratory of Ocean–Atmosphere Interaction and Climate in Universities of Shangdong, Ocean University of China, Qingdao* 266100

[2]*Key Laboratory of Meteorological Disaster, Nanjing University of Information Science and Technology, Ministry of Education, Nanjing* 210044

(Received 9 May 2014; revised 30 September 2014; accepted 8 October 2014)

ABSTRACT

An extreme rainstorm hit southern China during 13–17 December 2013, with a record-breaking daily rainfall rate, large spatial extent, and unusually long persistence. We examined what induced this heavy rainfall process, based on observed rainfall data and NCEP–NCAR reanalysis data through composite and diagnostic methods. The results showed that a Rossby waveguide within the subtropical westerly jet caused the event. The Rossby wave originated from strong cold air intrusion into the subtropical westerly jet over the eastern Mediterranean. With the enhancement and northward shift of the Middle East westerly jet, the Rossby wave propagated slowly eastward and deepened the India–Burma trough, which transported a large amount of moisture from the Bay of Bengal and South China Sea to southern China. Strong divergence in the upper troposphere, caused by the enhancement of the East Asian westerly jet, also favored the heavy rainfall process over Southeast China. In addition, the Rossby wave was associated with a negative-to-positive phase shift and enhancement of the North Atlantic Oscillation, but convergence in the eastern Mediterranean played the key role in the eastward propagation of the Rossby wave within the subtropical westerly jet.

Key words: subtropical westerly jet waveguide, southern China rainstorm, Rossby wave, India–Burma trough, North Atlantic Oscillation

Citation: Li, C., and J. L. Sun, 2015: Role of the subtropical westerly jet waveguide in a southern China heavy rainstorm in December 2013. *Adv. Atmos. Sci.*, **32**(5), 601–612, doi: 10.1007/s00376-014-4099-y.

1. Introduction

During 13–17 December 2013 an unusually heavy rainfall event affected Southeast Asia. It began over the northern Indochina Peninsular on 13 December, then separated northeastward to southern China, and ended on 18 December over the East China Sea and south of Japan (Fig. 1a). The heavy rainfall process was a disastrous weather event that had severe impacts on society. For example, related to the event, Thailand issued 23 extreme weather warnings during 11–16 December 2013, and the China Meteorological Administration (CMA) also issued many rainstorm alerts. Daily precipitation of above 100 mm was observed at many weather stations during this extreme rainfall process, and 160 weather stations recorded 6-h precipitation as exceeding 20 mm on a total of 257 separate occasions (Fig. 1a).

Many studies demonstrated the impacts of the North African–Asian (NAA) jet and the North Atlantic Oscillation (NAO) on Asian climate in winter (e.g. Syed et al., 2006; Feldstein and Dayan, 2008; Wen et al., 2009; Ni et al., 2010; Chen et al., 2013; Li et al., 2013), spring (e.g. Zhou, 2013) and summer (e.g. Yang et al., 2004). These previous studies focused mainly on the interannual and decadal timescales, with few paying attention to the synoptic scale. On the decadal timescale, Chen et al. (2013) found that the strength of the NAA jet is highly consistent with the frequency of cold air temperature extremes in China. Meanwhile, Li et al. (2013) demonstrated that the NAO can be used as a predictor of northern hemispheric mean temperature multidecadal variability with a lead time of 15–20 years. On the interannual timescale, the NAO can affect winter rainfall over central southwestern Asia (Syed et al., 2006), Israel (Feldstein and Dayan, 2008), and the tropical Indian Ocean (Gong et al., 2013) via the Rossby wave activity within the NAA jet (i.e. the NAA jet Rossby waveguide). In addition, the Rossby wave within the NAA jet, coupled with a strengthening of the NAA jet, can also influence cold air temperature extremes in China (Chen et al., 2013). Wen et al. (2009) reported that the frequent and persistent ice and snowstorms

* Corresponding author: LI Chun
Email: lichun7603@ouc.edu.cn

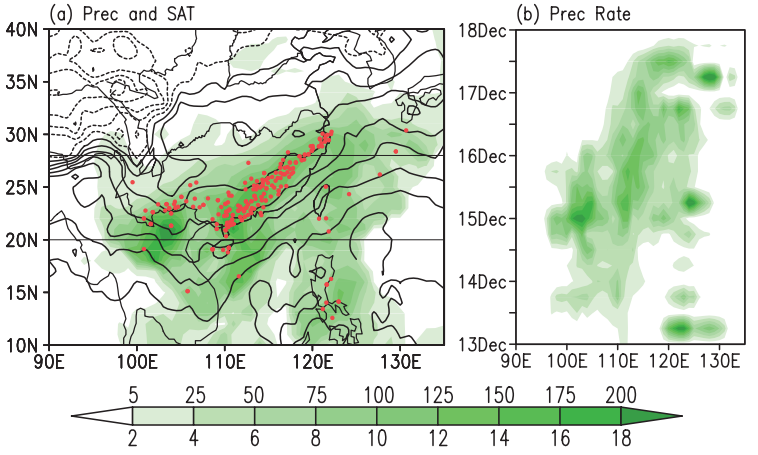

Fig. 1. (a) Total precipitation (mm) and mean SAT [contour interval (CI) = 4°C, black lines) during 13–17 December 2013. (b) Averaged six-hourly precipitation rate (mm) within 20°–28°N. The red dots in (a) are weather stations where the six-hourly precipitation rate exceeded 20 mm.

in southern China in the January of 2008 were closely linked with an anomalous enhancement of the NAA jet in the Middle East. Zhou et al. (2009) also reported synoptic-scale controls of persistent low temperature and icy weather over southern China in January 2008. The NAA jet exists with two strong centers—one in the Middle East called the Middle East jet (MEJ), and the other in East Asia called the East Asian jet (EAJ). The NAO may directly influence the MEJ in winter via western disturbances originating mostly from the Mediterranean (Syed et al., 2006). In general, such western disturbances propagate eastward to the Middle East and cease there in December because of the weak waveguide over the Arabian Sea and the lack of a low wavenumber boundary (Watanabe, 2004; Suo et al., 2008). The waveguide is stronger in January and February when upstream disturbances propagate easily in the eastward direction toward eastern Asia (Watanabe, 2004; Suo et al., 2008). These upstream western disturbances share a quasi-barotropic vertical structure and quasi-stationary Rossby waves (Watanabe, 2004; Suo et al., 2008; Suo and Ding, 2009). The role of convergence in the Mediterranean is very important for the downstream extension of the NAO in stimulating quasi-stationary Rossby waves along the NAA jet waveguide (Watanabe, 2004).

Our aim in the present study was to identify the mechanism that caused the unusually heavy rainfall process over southern China in December 2013. A brief description of the data and methods is provided in section 2. In section 3, the major results are presented, including an analysis of the synoptic conditions, anomalous Rossby wave source, and teleconnection with the NAO, as well as an explanation of the proposed mechanism involved. Further discussion and a summary of our findings are provided in section 4.

2. Data and methods

The rainfall and surface air temperature (SAT) data used in the study were provided by the Meteorological Information Comprehensive Analysis and Process System (MICAPS). Specifically, the data were obtained from the data server at the Department of Marine Meteorology, Ocean University of China. MICAPS is a high-speed technologically-advanced processing, display, and telecommunication network used for nationwide weather services in China. The MICAPS surface data are satellite-broadcasted to all meteorological bureaus every three hours by the CMA. The rainfall data have a temporal resolution of six hours. We chose the rainfall and SAT data that covered the region (10°–40°N, 90°–135°E). The other atmospheric data were from the National Centers for Environmental Prediction–National Center for Atmospheric Research (NCEP–NCAR) reanalysis dataset (Kalnay et al., 1996), including daily geopotential height, wind, vertical velocity, specific humidity etc. The daily NAO index data were taken from the NOAA Climate Prediction Center (http://www.cpc.ncep.noaa.gov/products/precip/CWlink/pna/nao.shtml). World time was used to match with the NCEP–NCAR reanalysis data.

The synoptic conditions of this heavy rainfall process were demonstrated by using composite weather maps during 14–17 December 2013. To confirm the wave-like pattern, velocity potential was calculated by solving the Poisson equation,

$$\Delta\chi = D\,, \tag{1}$$

where χ is velocity potential and D is divergence. Divergent wind can be written by

$$\boldsymbol{V}_\chi = \nabla\chi\,, \tag{2}$$

and then the vertical structure of the subtropical waveguide in the NAA jet could be examined. Horizontal stationary wave activity flux was calculated to demonstrate the propagation of wave energy, based on the method of Plum (1985):

$$\boldsymbol{F} = p\cos\phi \begin{pmatrix} \dfrac{1}{2a^2\cos^2\phi}\left[\left(\dfrac{\partial\psi'}{\partial\lambda}\right)^2 - \psi'\dfrac{\partial^2\psi'}{\partial\lambda^2}\right] \\ \dfrac{1}{2a^2\cos^2\phi}\left(\dfrac{\partial\psi'}{\partial\lambda}\dfrac{\partial\psi'}{\partial\phi} - \psi'\dfrac{\partial^2\psi'}{\partial\lambda\partial\phi}\right) \end{pmatrix}. \tag{3}$$

Here, p is a pressure coefficient (pressure/1000 hPa), ψ' is the perturbation stream function, and a is Earth's radius.

In addition, daily time–longitude cross sections were plotted to demonstrate the propagation of the subtropical Rossby wave within the NAA. Correlation and regression of geopotential height against the NAO index were used to examine whether wave activity was related to the NAO activity. Lastly, another similar rainfall event that took place during 1–3 December 1994 was analyzed to confirm the subtropical waveguide mechanism in winter rainfall over southern China.

3. Results

3.1. *Synoptic analysis*

During 13–17 December 2013 an unusually heavy rainfall event affected Southeast Asia, with maximum daily precipitation above 100 mm (Fig. 1a). It is not common in winter to see a rainfall process in this region with such remarkable spatial extent and persistence. Six-hourly precipitation of greater than 20 mm was observed at many weather stations, with extremes even exceeding 100 mm. From the six-hourly precipitation averaged within 20°–28°N, the heavy rainfall began over the Indochina Peninsula, then spread northeastward to southern China, and ended over southeast Japan (Fig. 1b). As the heavy rainfall mainly occurred during 14–17 December 2013, we composited weather maps of this period to examine the synoptic conditions. The NCEP–NCAR reanalysis data also captured the heavy rainfall in terms of its spatial distribution and long-lasting temporal evolution, although with a rainfall rate that was stronger than observed (not shown). Therefore, the NCEP–NCAR reanalysis data were used to understand this unusually heavy rainfall process. To examine the synoptic conditions of the heavy rainfall process, we present the composite maps of divergence and zonal wind at 200 hPa (Fig. 2a), geopotential height and vertical velocity at 500 hPa, total moisture transportation (Fig. 2b), geopotential height, wind and divergence at 850 hPa (Fig. 2c).

In the upper troposphere, a very long and strong NAA jet meandered from the subtropical eastern Atlantic and northern Africa, stretching eastward to eastern Asia and the northwestern Pacific (Fig. 2a). A wave-like divergence/convergence was constrained within the NAA jet. The major divergences existed in northwestern Africa, Uzbekistan and southeastern China. The major convergences located in the subtropical northeastern Atlantic, northeastern Africa, southern Tibet, and North China–Japan. The strongest divergence (convergence) could be identified in southeastern Tibet (southeastern Asia), located in the southeastern export region (southwestern import region) of the EMJ (EAJ) (Fig. 2a). In the middle troposphere, a strong westerly synoptic system between the Icelandic low and the Azores high was separated into two branches. The northern branch meandered eastward with large meridional amplitude and established a northeast–southwest blocking system over Lake Baikal, while the southern branch stretched southeastward, constrained within 15°–35°N, accompanied by clear ascending and descending motion (Fig. 2b). In addition, two subtropical highs existed over the Arabian Sea and the northwestern Pacific, respectively, and the two branches seemed to converge over eastern Asia (Fig. 2b). The ascending (descending) motion in the middle troposphere was coupled with divergence (convergence) in the upper troposphere (Fig. 2a vs. 2b). In the lower troposphere, the north branch of the westerly synoptic system was also obvious, similar to that in the middle troposphere. However, the south branch became weaker with weak cyclonic (anticyclonic) wind along the NAA jet, but the subtropical high over the northwestern Pacific was also pronounced (Fig. 2c). Another feature was cold advection with northerly wind over northeastern Africa (eastern Asia), coupled with upper tropospheric convergences and mid-troposphere southwest–northeast (west–east) troughs (Figs. 2a and c), which induced the propagation of Rossby energy southeastward from the midlatitudes to the NAA jet (Li, 1988). A strong convergence region over Southeast Asia was caused by East Asian northerly wind and the northwestern Pacific subtropical high (Fig. 2c). The convergence in the lower troposphere, coupled with the divergence south of the EAJ entrance in the upper troposphere, induced strong atmospheric convection that caused the heavy rainfall over Southeast Asia.

The velocity potential and divergent wind anomalies, as contrasted with the climatological state during the period 1981–2010, were calculated to further demonstrate the wave-like convergence (divergence) in the upper (200 hPa) and lower (850 hPa) troposphere (Fig. 3). In the upper troposphere, distinct tow branches of wave-like convergence (divergence) existed in the high and the subtropical latitudes. The south branch was more distinct, which was consistent with the composite weather maps (Fig. 3a vs. Figs. 2a and b). Interestingly, the anomalous convergence (divergence) corresponded to the anomalous north (south) wind. Therefore, meridional wind anomalies could represent this wave-like activity. In the lower troposphere, wave-like convergence (divergence) in the high latitudes was also evident. However, the wave-like convergence (divergence) was weaker in the subtropical latitudes (Fig. 3a vs. Fig. 3b). The divergence (convergence) anomaly that was centered over the eastern Mediterranean (southeastern Asia) was still obvious, corresponding to the convergence (divergence) (Fig. 2a) and strong descending (ascending) vertical motion there (Fig. 2b).

To reveal the vertical structure of the wave train within the NAA jet, we composited the vertical–longitude section of daily geopotential height anomalies (based on the climatology during 1981–2010) along 20°–35°N during 14–17 December 2013 (Fig. 4a). The wave train within the NAA jet had a quasi-barotropic vertical structure and became stronger in the upper layer than in the lower layer of the troposphere. The wave-like geopotential height anomalies were strongest at 300–200 hPa. The wave train was similar to the Rossby waveguide pattern (Branstator, 2002). Therefore, we composited daily geopotential height anomalies at 250 hPa dur-

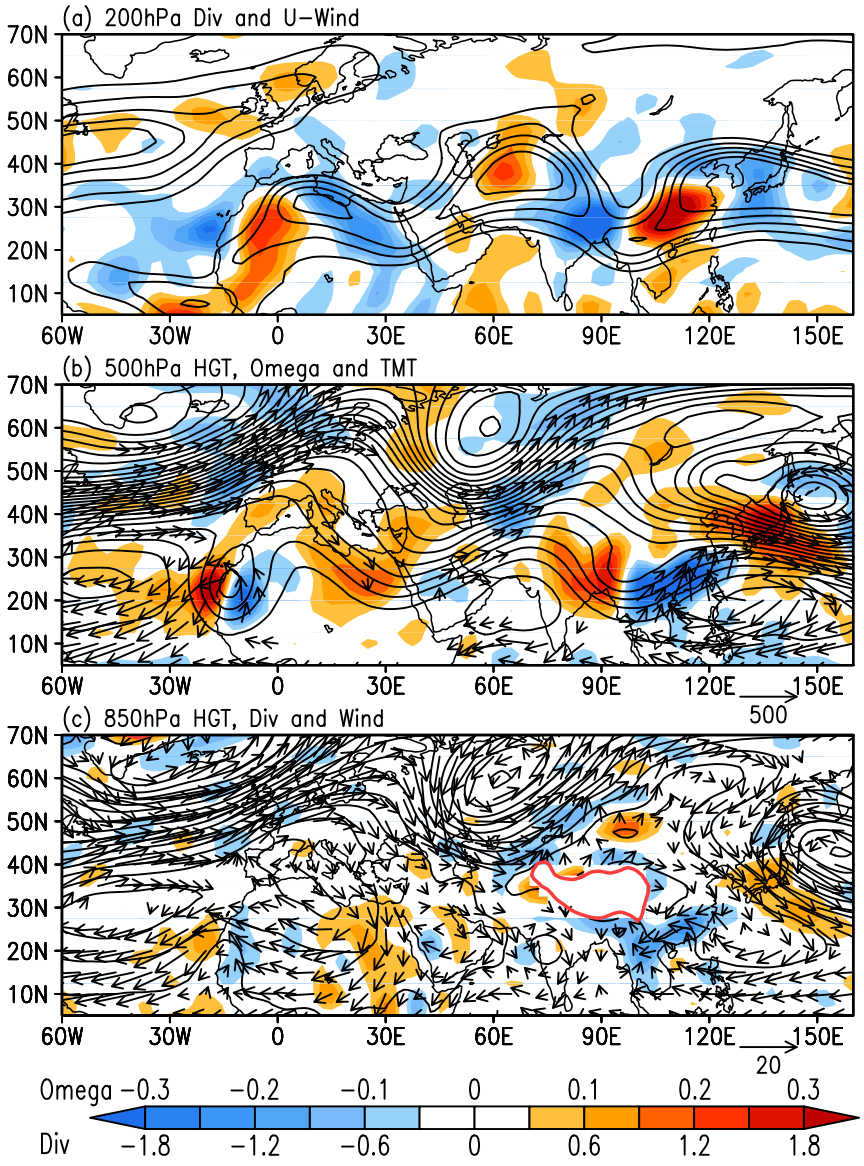

Fig. 2. Composite weather maps during 14–17 December 2013: (a) divergence (shaded, 10^{-5} s^{-1}) and zonal wind (CI = 20, 30, . . . , 60 m s^{-1}) at 200 hPa; (b) geopotential height (contours, CI = 40 gpm) and vertical velocity (shaded, Pa s^{-1}) at 500 hPa and total moisture transport (vectors, g m kg^{-1} s^{-1}); (c) geopotential height (contours, CI = 40 gpm), divergence (shaded, 1.0×10^{-5} s^{-1}) and wind (vectors, m s^{-1}) at 850 hPa. The red line in (c) denotes the topographic height of 3000 m.

ing 14–17 December 2013 and calculated its wave activity flux (Fig. 4b), based on the method of Plum (1985). Two obvious wave-like geopotential anomalies existed to the north and south of 40°N, and the north branch was stronger than the south branch. The wavelength of the north branch was also longer than that of the south branch. The centers of the north branch of the Rossby wave were located over the North Atlantic and northern Kazakhstan with negative geopotential height anomalies, but with positive geopotential height anomalies they were located over Europe and northeastern Asia. The north branch of the Rossby wave propagated from the North Atlantic to western Lake Baikal and was seemingly blocked by a blocking high over Lake Baikal, the development and persistence of which was favored by the energy convergence there (Luo, 2005). The blocking high was able to enhance the genesis of an air temperature front and cause a strong meridional temperature gradient over southeastern Asia (Fig. 1a). The centers of the south branch of the Rossby wave were located over the subtropical North Atlantic, Algeria, north Arabian Sea, and Korean Peninsula with positive geo-potential height anomalies, but with negative geopotential height anomalies they were located over northwestern Africa, the Arabian Peninsula, the northern Indochina Peninsula, and northwestern Pacific. The south branch of the

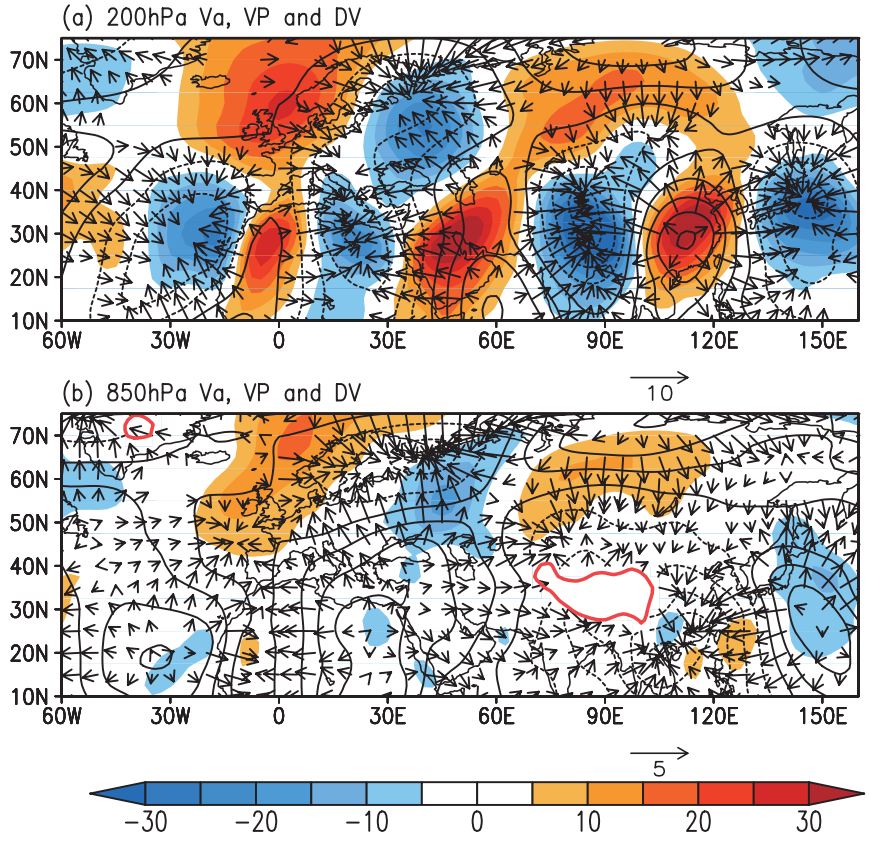

Fig. 3. Composite anomalous meridional wind (shaded, m s^{-1}), velocity potential (contours, CI = 2×10^5 m^2 s^{-1}) and divergent wind (vectors, m s^{-1}) during 14–17 December 2013 at (a) 200 hPa and (b) 850 hPa.

Rossby wave propagated from the subtropical northern Atlantic and northern Africa to southeastern Asia and the northwestern Pacific, constrained within the climatological waveguide of the NAA jet. In addition, the anomalous geopotential height over the North Atlantic showed a strong negative anomaly in the high latitudes and a positive anomaly in the subtropical latitudes, which resembled the positive phase of the NAO (discussed later).

3.2. *Anomalous Rossby wave source*

Since the subtropical wave train was similar to the "waveguide pattern" (Branstator, 2002) and it had a quasi-barotropic vertical structure, a barotropic vorticity equation could be used to understand it. For this purpose, we also calculated the Rossby wave source following Watanabe (2004). The wave source was computed following Sardeshmukh and Hoskins (1998),

$$S = -\nabla \cdot (\boldsymbol{V}_\chi \xi) \,, \tag{4}$$

where $\xi = \zeta + f$ is the absolute vorticity and $\boldsymbol{V}_\chi$ the divergent wind calculated from the velocity potential field.

The anomalous wave source could be decomposed into four terms,

$$S = -\nabla \cdot (\overline{\boldsymbol{V}}_\chi \zeta') - \nabla \cdot (\boldsymbol{V}'_\chi \overline{\zeta}) - \nabla \cdot (f \boldsymbol{V}'_\chi) - \nabla \cdot (\boldsymbol{V}'_\chi \zeta') \,, \tag{5}$$

where the overbars are the climate state during 1981–2010 and the primes denote anomalies subtracted from the climate state.

The Rossby wave source is shown in Fig. 5. The total wave source also demonstrated the wave train within the NAA jet (Fig. 5a). The wave source propagated eastward from the North Atlantic and eastern Mediterranean from the daily anomalous wave source (not shown). This means that the south branch of the Rossby wave originated from the eastern Mediterranean and the wave sources caused by the propagation of the Rossby wave served as a relay source. From the decomposed wave source terms, the first two terms—associated with relative vorticity—were very weak (Figs. 5b and c); while the third term—associated with geostrophic vorticity—was dominant and very similar to the total wave source (Fig. 5a vs. Fig. 5d). The fourth nonlinear term represented a smaller-scale and higher-order term (Fig. 5e); its value was also smaller than the third term. Therefore, the fourth nonlinear term could be neglected.

3.3. *Teleconnection with NAO activity*

Since the geopotential height anomaly demonstrated the NAO pattern in the North Atlantic, the question arose as to whether the two Rossby waves propagating slowly eastward were related to daily NAO activity. To address this, geopoten-

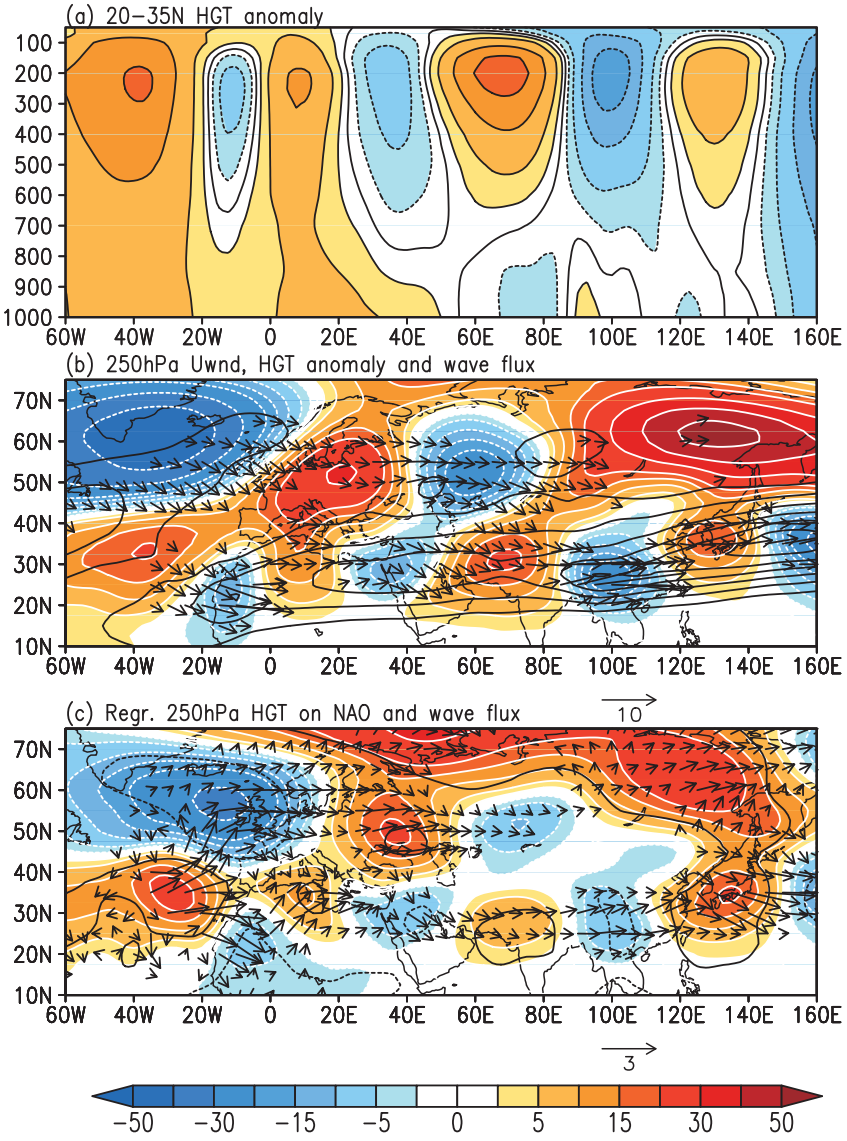

Fig. 4. (a) Composite vertical structure of anomalous geopotential height (10 gpm) averaged in 20°–35°N during 14–17 December 2013. (b) Composite maps of zonal wind (contours, m s^{-1}), anomalous geopotential height (shaded, 10 gpm) and its stationary wave activity flux (vectors, m^2 s^{-2}). (c) Regression of geopotential height (shaded, 10 gpm) on daily NAO indices during 1–21 December 2013 and its stationary wave activity flux (vectors, m^2 s^{-2}). The black contours in (c) represent statistical significance at the 0.05 confidence level.

tial height was regressed against daily NAO index during 1–20 December 2013 and its wave activity flux was calculated based on the regression pattern (Fig. 4c). The regression pattern showed spatial similarity with the composited weather map during 14–17 December 2013, with a spatial correlation coefficient of 0.72 (Figs. 4b and c). The wave activity flux also showed spatial similarity. In addition, we also repeated a single-point regression of the geopotential height anomaly on the Icelandic low (60°N, 30°W) and Azores high (30°N, 35°W) (not shown). The single-point regressions also shared the same spatial similarity with the composited weather map. Their spatial cross-correlation coefficients are listed in Table 1. These regressions and their wave activity flux analyses implied that this unusually heavy rainfall event over Southeast Asia was related to the remote influence of NAO activity. As

Table 1. Spatial correlation between the composited geopotential height anomaly (CGPHA) and the regression of the daily geopotential height anomaly against the NAO, Iceland low (IL), Azores high (AH) and AH-IL indices.

	NAO	IL	AH	AH-IL
CGPHA	0.72	−0.76	0.73	0.76
AH-IL	0.87	−0.99	0.99	
AH	0.86	−0.96		
IL	−0.86			

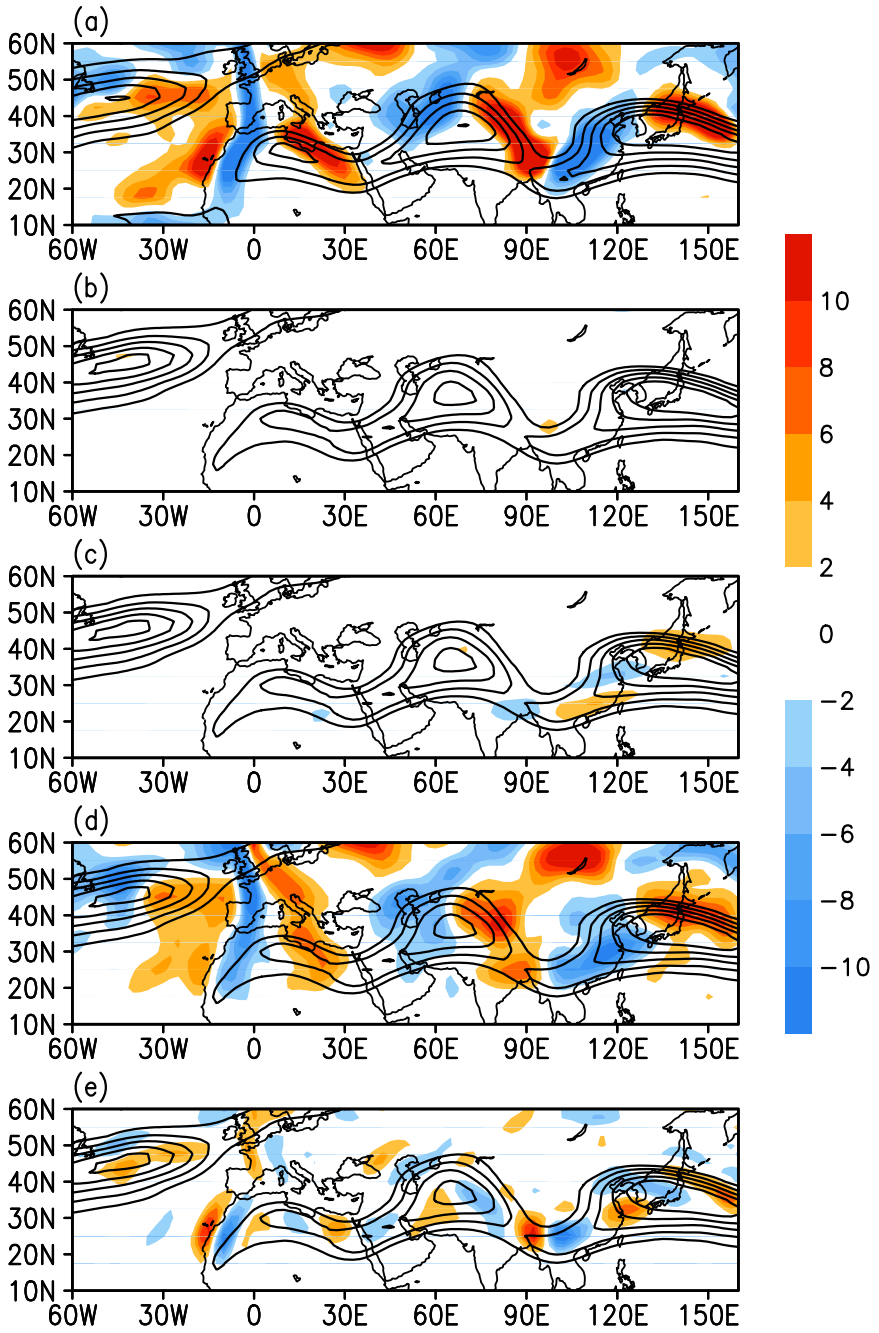

Fig. 5. Rossby wave source anomalies (shaded, 10^{-10} s^{-2}) and the climatological zonal westerly jet (contours: CI = 30, 40, 50, 60 and 70 m s^{-1}): (a) $-\nabla\cdot(\boldsymbol{V}_\chi\xi)$; (b) $-\nabla\cdot(\overline{\boldsymbol{V}}_\chi\zeta')$; (c) $-\nabla\cdot(\boldsymbol{V}'_\chi\overline{\xi})$; (d) $-\nabla\cdot(f\boldsymbol{V}'_\chi)$; (e) $-\nabla\cdot(\boldsymbol{V}'_\chi\xi')$.

to what caused the phase shifts and amplitude enhancement of the NAO, however, is beyond the scope of the current paper.

3.4. *Propagation of the subtropical Rossby wave*

To further examine the propagation of the south branch of the Rossby wave, we plotted time–latitude sections of anomalous meridional wind at 200 hPa (Fig. 6a) and velocity potential at 200 hPa (Fig. 6b) and 850 hPa (Fig. 6c) averaged within 10°–30°E band, and time–longitude sections of anomalous meridional wind at 200 hPa (Fig. 6d), velocity potential at 200 hPa (Fig. 6e) and 850 hPa (Fig. 6f), and geopotential height anomalies and wave activity flux averaged within 20°–35°N (Fig. 7a).In terms of the origin of the south branch, a northerly wind anomaly over continental Europe was enhanced and extended from the high latitudes to the Mediterranean on 11 December, achieving its maximum strength on 13 December and persisting until 15 December before weak-

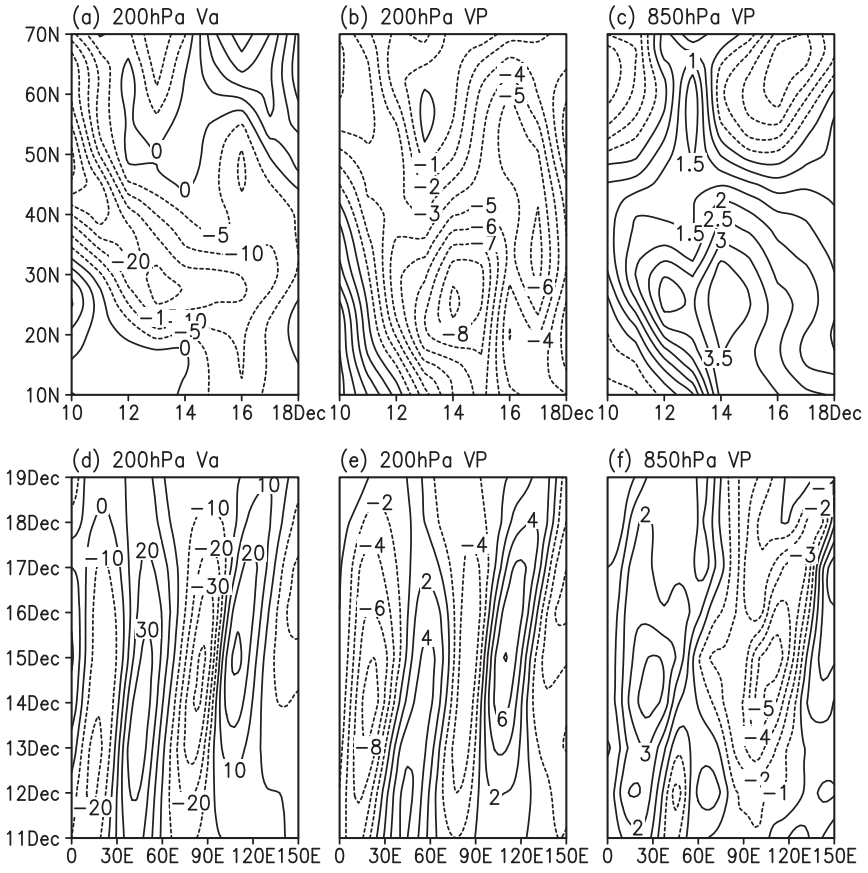

Fig. 6. Latitude–time section of (a) anomalous meridional wind (m s^{-1}) at 200hPa, (b) velocity potential (10^5 m^2 s^{-1}) at 200 hPa, and (c) velocity potential (10^5 m^2 s^{-1}) at 850 hPa, averaged over 10°–30°E. Panel (d–f) is the same as (a–c), but averaged over 20°–35°N.

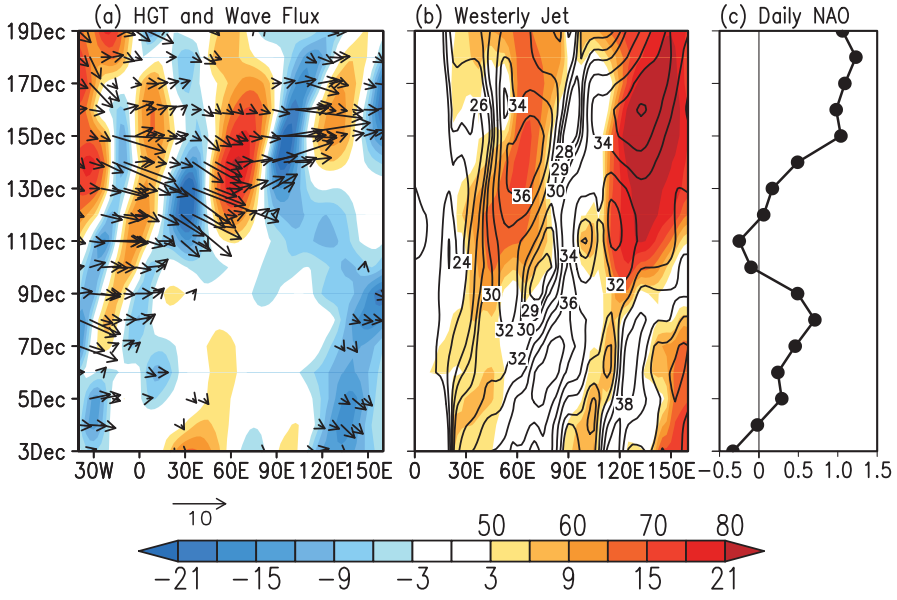

Fig. 7. Longitude–time sections of (a) geopotential height anomaly (shaded, 10 gpm) and stationary wave activity flux (vectors, m^2 s^{-2}) averaged over 20°–35°N, and (b) maximum zonal wind speed (shaded, m s^{-1}) of the subtropical westerly jet and its meridional position (contours, N) at 250 hPa. (c) Daily NAO index.

ening (Fig. 6a). Accompanied by changing anomalous northerly wind, convergence over the Mediterranean began on 12 December, achieving its maximum on 14 December before weakening after 15 December at 200 hPa (Fig. 6b). Anomalous divergence at 850 hPa followed the convergence at 200 hPa via Ekman pumping and low-level friction (Fig. 6c). Convergence in the upper layers and divergence in the lower layers caused strong downward descending motion over the Mediterranean (Fig. 2b). This implied that convergence over the Mediterranean was induced by strong cold air intrusion, caused by anomalous enhanced northerly wind.

The NAO had a similar negative–positive phase shift and was enhanced before and after 10 December (Fig. 7c), but the Rossby wave had not propagated eastward and ceased over northwestern Africa before 10 December due to the weak NAA jet and positive NAO amplitude without cold air intrusion and significant convergence over the eastern Mediterranean. After 10 December, however, the Rossby wave had propagated eastward to eastern Asia and the northwestern Pacific with strong cold air intrusion and convergence over the eastern Mediterranean. This tells us that some of the NAO activity could have extended downstream and affected the weather in Southeast Asia, but only because it was accompanied by strong convergence over the Mediterranean (Watanabe, 2004). Therefore, strong convergence over the Mediterranean, induced by strong cold air intrusion, played a key role for the extreme heavy rainfall process in southeastern China during 14–17 December 2013.

Propagation of the south branch may trace back to 11 December 2013 (Fig. 7a). The Rossby wave within the NAA jet propagated eastward to southern Tibet and was enhanced during 11–12 December (Fig. 7a), when the NAO phase shifted from negative to positive and the amplitude of the NAO enhanced (Fig. 7c). During this period, the Middle East westerly jet strengthened and shifted northward (Fig. 7b), which favored cold air intrusion from the eastern Mediterranean (Figs. 6a and d) and convergence there (Figs. 6b and e). The wave propagated eastward to the northern Indochina Peninsular and enhanced the India–Burma trough on 13 December, when rainfall began in the region with persistent strong cold air intrusion from the eastern Mediterranean (Figs. 6a and d) and distinct convergence (divergence) in the upper (lower) troposphere (Figs. 6b and c, Figs.6e and f). It then moved to southeastern China and caused the heavy rainfall over Southeast Asia (Fig. 1b), accompanied by local-scale strong convection induced by strong divergence (convergence) in the upper (lower) troposphere (Figs. 6ef) and moisture convergence over Southeast Asia (Fig. 2b). Propagation of the Rossby wave ceased on 18 December and led to a termination of the heaviest part of the rainfall process, with a southward shift of the EMJ (Fig. 7b) and a halt to the cold air intrusion over the eastern Mediterranean (Fig. 6d).

3.5. *Proposed mechanism*

Based on the above analyses, a schematic illustration of the subtropical westerly jet waveguide that affected this heavy rainfall process in southern China is shown in Fig. 8. An anomalous high ridge over west Europe enhanced the northerly winds extending southward. The anomalous northerly winds induced descending cold air and convergence over the eastern Mediterranean, named "western disturbance" (Syed et al., 2006). Accompanying the enhancement and northward shift of the MEJ, the western disturbance propagated eastward to Southeast Asia along the NAA jet and enhanced the India–Burma trough. The India–Burma trough then strengthened the transportation of moisture from the

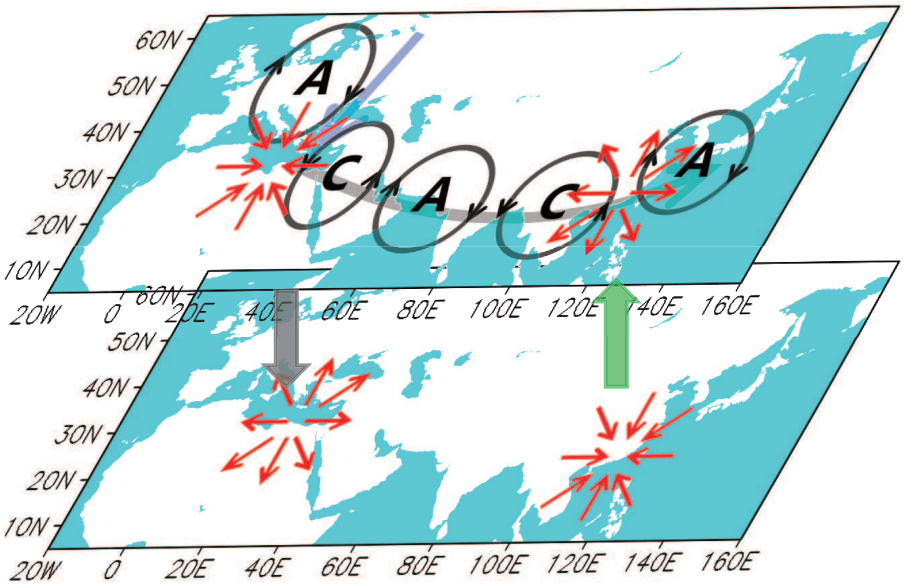

Fig. 8. Schematic illustration of the subtropical westerly jet waveguide affecting heavy rainfall in southern China.

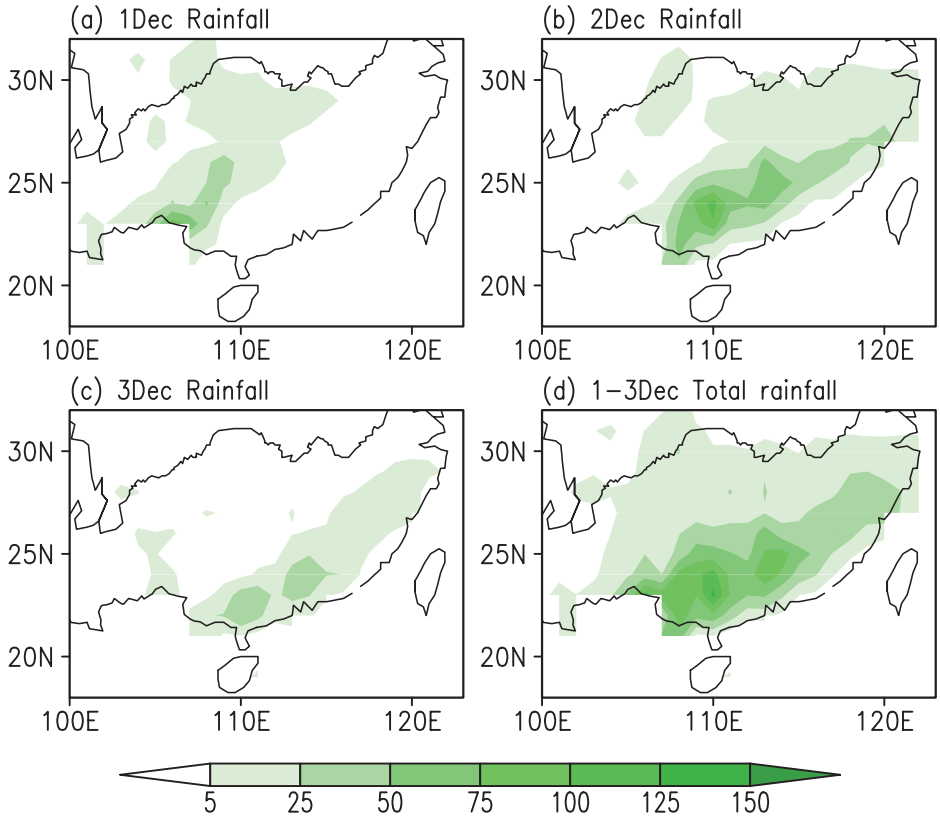

Fig. 9. (a–c) Daily precipitation (mm) for 1–3 December 1994, respectively. (d) Total precipitation (mm) during 1–3 December 1994.

Bay of Bengal and the South China Sea toward southeastern China. Meanwhile, strong divergence induced by the EAJ in the upper troposphere and convergence induced by the enhanced India–Burma trough induced strong convention over southeastern China, which ultimately resulted in the extreme (in both spatial and temporal terms) heavy rainfall process during 14–17 December 2013.

4. Summary and discussion

An extreme heavy rainfall process was investigated based on station-observed rainfall, SAT data and NCEP–NCAR reanalysis data. This event, which was unusual both in terms of its large spatial extent and remarkable persistence, was caused by strong convection induced by strong divergence (convergence) in the upper (lower) troposphere in the south of the westerly EAJ entrance. An enhanced India–Burma trough, induced by the Rossby wave propagating from the Mediterranean, favored abundant water vapor transportation from the Bay of Bengal and the South China Sea.

This extreme heavy rainfall process was primarily caused by a Rossby wave propagating slowly and eastwardly from North Africa to southeastern Asia within the subtropical westerly jet. The Rossby wave originated from strong convergence in the eastern Mediterranean–induced intrusion of midlatitude cold air, characterized by a quasi-barotropic vertical structure that was more distinct in the upper than the lower troposphere. Therefore, the Rossby wave resembled a waveguide pattern within the NAA jet. Although the Rossby wave was associated with daily NAO activity, strong convergence in the eastern Mediterranean induced by cold air intrusion played the key role in the eastward propagation of the Rossby wave.

But is it robust that the Rossby wave train caused the large spatial extent and extraordinary persistence of this rainfall process? To answer this, we also examined the mechanism involved in another rainfall process during 1–3 December 1994. The rainfall began in northwestern Yunnan and southwestern Guizhou on 1 December and then spread eastward to southeastern China on 2 December (Figs. 9a and b). On 3 December the rainfall process weakened and ended (Fig. 9c). The large spatial extent of the rainfall process in December 1994 was similar to that of the heavy rainfall process during 14–17 December 2013, but the total precipitation amount was less (Figs. 1a and 9d). The weather conditions of the rainfall process during 1–3 December 1994 were also similar to those during 13–17 December 2013 (Figs. 10a and 2b). In the mid–high latitudes, two large ridges existed over Western Europe and Lake Baikal, and three major troughs existed over the eastern North Atlantic, Ural mountains, and northeastern Asia (Fig. 10a). In the subtropical region, relatively short troughs (ridges) were accompanied by wave-like ascending (descending) motion, and two subtropical highs existed over the Arabian Sea and Northwestern Pacific (Fig.

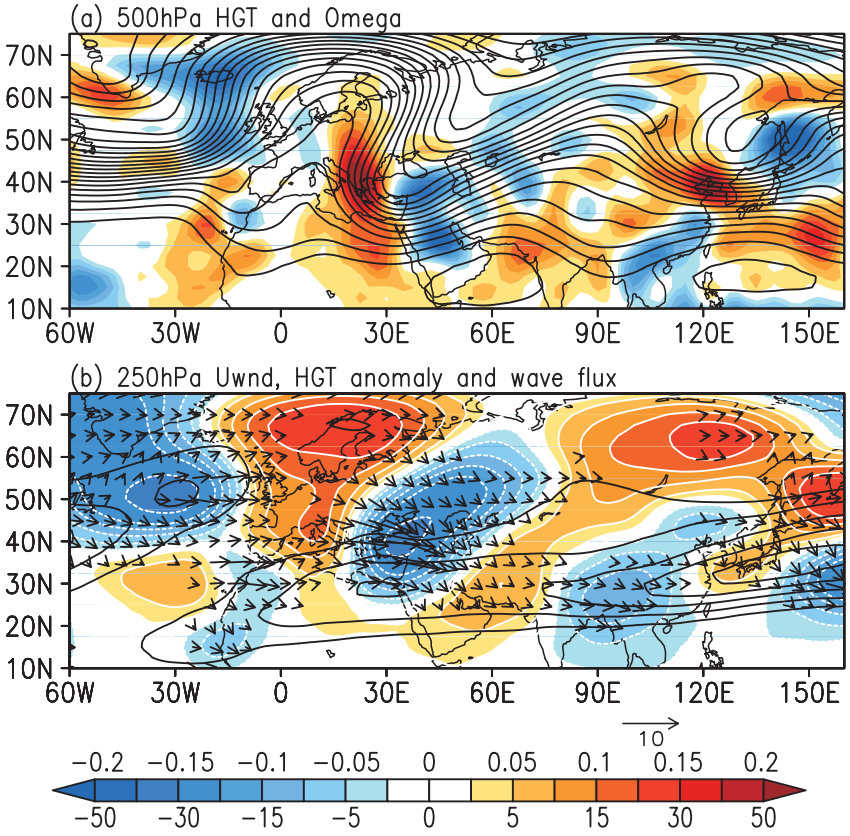

Fig. 10. (a) Composite geopotential height (contours, CI = 40 gpm) and vertical velocity (shaded, Pa s^{-1}) at 500 hPa during 1–3 December 1994. (b) Composite maps of zonal wind (contours, m s^{-1}), geopotential height anomalies (shaded, 10 gpm) and its stationary wave activity flux (vectors, m^2 s^{-2}) at 250 hPa during 1–3 December 1994.

10a). In the upper troposphere, the wave-like geopotential height anomalies and Rossby wave activity flux were also similar to those in the heavy rainfall event during 13–17 December 2013 (Figs. 10b and 4b). The difference was that the Middle East westerly jet was weaker in the 1–3 December 1994 event (Figs. 10b and 4b), which favored the weaker subtropical waveguide in spite of stronger cold air intrusion over the eastern Mediterranean.

From the above analysis and discussion, the waveguide within the NAA jet could be a key mechanism leading to rainfall processes in South China that are characterized by a large spatial extent and extraordinary persistence. However, because of a lack of historical daily rainfall data, only two rainfall processes were analyzed in this study. The robustness of the mechanism should be further verified using more rainfall cases as well as model simulations. If the mechanism is proven robust, it could help in the forecasting of such rainfall processes over South China in winter.

Acknowledgements. This work was supported by the National Natural Science Foundation of China (NSFC) (Grant Nos. 41276002 and 41130859), the National Basic Research Program of China (Grant Nos. 2012CB955603 and 2013CB956201), the NSFC–Shandong Joint Fund for Marine Science Research Centers (Grant No. U1406401), and the Fund for Open Research Programs of the Key Laboratory of Meteorological Disaster (Nanjing University of Information Science and Technology), Ministry of Education (KLME1301).

REFERENCES

Branstator, G., 2002: Circumglobal teleconnections, the jet stream waveguide, and the North Atlantic Oscillation. *J. Climate*, **15**, 1893–1910.

Chen, H.-S., L. Liu, and Y.-J. Zhu, 2013: Possible linkage between winter extreme low temperature events over China and synoptic-scale transient wave activity. *Sci. China Ser.* (*D*), **56**, 1266–1280.

Feldstein, S. B., and U. Dayan, 2008: Circumglobal teleconnections and wave packets associated with Israeli winter precipitation. *Quart. J. Roy. Meteor. Soc.*, **134**, 455–467.

Gong, D.-Y., Y.-Q. Gao, D. Guo, R. Mao, J. Yang, M. Hu, and M.-N. Gao, 2013: Interannual linkage between Arctic/North Atlantic Oscillation and tropical Indian Ocean precipitation during boreal winter. *Climate Dyn.*, **42**, 1007–1027, doi: 10.1007/s00382-013-1681-4.

Kalnay, E., and Coauthors, 1996: The NCEP/NCAR 40-year reanalysis project. *Bull. Amer. Meteor. Soc.*, **77**, 437–471.

Li, C.-Y., 1988: Frequent activity of East Asian trough and El Nino

onset. *Sci. China Ser.* (*B*), **31**, 667–674. (in Chinese)

Li, J., C. Sun, and F.-F. Jin, 2013: NAO implicated as a predictor of Northern Hemisphere mean temperature multidecadal variability. *Geophys. Res. Lett.*, **40**, 5497–5502.

Luo, D., 2005: A barotropic envelope Rossby soliton model for block-eddy interaction. Part II: Role of westward-traveling planetary waves. *J. Atmos. Sci.*, **62**, 22–40.

Ni, D.-H., Z.-B. Sun, Z.-X. Li, G. Zeng, and W.-T. Deng, 2010: Relation of Middle East jet stream and China climate anomaly in winter. *Scientia Meteorologica Sinica*, **30**, 301–307. (in Chinese)

Plumb, R. A., 1985: On the three-dimensional propagation of stationary waves. *J. Atmos. Sci.*, **42**, 217–229.

Sardeshmukh, P. D., and B. J. Hoskins, 1988: The generation of global rotational flow by steady idealized tropical divergence. *J. Atmos. Sci.*, **45**, 1228–1251.

Suo, M.-Q., and Y.-H. Ding, 2009: The structures and evolutions of the wintertime southern branch trough in the subtropical westerlies. *Chinese J. Atmos. Sci.*, **33**, 425–442. (in Chinese)

Suo, M.-Q., Y.-H. Ding, and Z.-Y. Wang, 2008: Relationship between Rossby wave propagation in southern branch of westerlies and the formation of the southern branch trough in wintertime. *J. Appl. Meteor. Sci.*, **19**, 731–740. (in Chinese)

Syed, F. S., F. Giorgi, J. S. Pal, and M. P. King, 2006: Effect of remote forcings on the winter precipitation of central southwest Asia Part 1: Observations. *Theor. Appl. Climatol.*, **86**, 147–160.

Watanabe, M., 2004: Asian jet waveguide and a downstream extension of the North Atlantic Oscillation. *J. Climate*, **17**, 4674–4691.

Wen, M., S. Yang, A. Kumar, and P.-Q. Zhang, 2009: An analysis of the Large-Scale climate anomalies associated with the snowstorms affecting China in January 2008. *Mon. Wea. Rev.*, **137**, 1111–1131.

Yang, S., K.-M. Lau, S.-H. Yoo, J. L. Kinter, K. Miyakoda, and C.-H. Ho, 2004: Upstream subtropical signals preceding the Asian summer monsoon circulation. *J. Climate*, **17**, 4213–4229.

Zhou, B.-T., 2013: Weakening of winter North Atlantic Oscillation signal in spring precipitation over southern China. *Atmos. Oceanic Sci. Lett.*, **6**, 248–252.

Zhou, W., J. C. L. Chan, W. Chen, J. Ling, J. G. Pinto and Y.-P. Shao, 2009: Synoptic-scale controls of persistent low temperature and icy weather over southern China in January 2008. *Mon. Wea. Rev.*, **137**, 3978–3991.